ISSN 2071-2898 (Print)
ISSN 2071-2901 (Online)

Ovchinnikov M. Y., Roldugin D.S., Testani P.

Spin-stabilized satellite with Sun-pointing active magnetic attitude control system

Recommended form of bibliographic references

Ovchinnikov M. Y., Roldugin D.S., Testani P. Spin-stabilized satellite with Sun-pointing active magnetic attitude control system // Keldysh Institute Preprints. 2012. No. 4. 31 p.
URL: http://library.keldysh.ru/preprint.asp?id=2012-4&lg=e

Publications based on the preprint

D. Roldugin, P. Testani, Spin-stabilized satellite magnetic attitude control scheme without initial detumbling // Acta Astronautica, 2014, V. 94, pp. 446-454
DOI: 10.1016/j.actaastro.2013.01.011
URL: http://www.sciencedirect.com/science/article/pii/S0094576513000234

KELDYSH INSTITUTE OF APPLIED MATHEMATICS
RUSSIAN ACADEMY OF SCIENCE

M.Yu. Ovchinnikov, D.S. Roldugin, P. Testani

Spin-stabilized satellite with Sun-pointing active magnetic attitude control system

Moscow
2012

Spin-stabilized satellite with Sun-pointing active magnetic attitude control system. M.Yu. Ovchinnikov, D.S. Roldugin, P. Testani. The Keldysh Institute of Applied Mathematics of Russian Academy of Sciences, 2012, 31p., 12 items of bibliography, 22 figures

The angular motion of an axisymmetrical satellite equipped with the active magnetic attitude control system is considered. Dynamics of the satellite is analytically studied on the whole control loop. Two coarse sun-pointing algorithms and nutation damping are studied. Fine sun-pointing algorithm is implemented last. Two different algorithms are proposed. Active magnetic attitude control system time-response with respect to its parameters is analyzed, orbit inclination is of particular interest. Numerical simulation is carried out.

Key words: active magnetic attitude control, spin-stabilized satellite, averaged geomagnetic field model, time-response, sun-pointing

Спутник с активной магнитной системой ориентации, реализующей его разворот на Солнце. М.Ю. Овчинников, Д.С. Ролдугин, П. Тестани. ИПМ им. М.В.Келдыша РАН, Москва, 2012 г., 31с., библиография: 12 наименований, 22 рисунков

Рассматривается осесимметричный спутник, оснащенный активной магнитной системой ориентации. В рамках осредненной модели геомагнитного поля аналитически исследуются два алгоритма грубой ориентации на Солнце, используемые совместно с алгоритмом гашения нутационных колебаний. После них используется один из двух различных алгоритмов точной ориентации на Солнце. Рассматривается зависимость быстродействия активной магнитной системы от параметров задачи, в первую очередь – от наклонения орбиты. Результаты подтверждаются численным моделированием.

Ключевые слова: магнитная система ориентации, спутник, стабилизируемый собственным вращением, осредненная модель магнитного поля Земли, быстродействие системы ориентации, ориентация на Солнце

Introduction

Spin stabilization is a common way to maintain a satellite attitude. Satellite acquires the properties of a gyroscope while it is spinned around the axis of symmetry with a high angular velocity. In our recent work [1] attitude control system (ACS) functioning was divided into three stages: nutation damping, spinning around the axis of symmetry, reorientation of the axis in the inertial space. These stages may be combined. To conduct the whole control circle, satellite must be equipped with an active ACS to control its angular velocity and attitude. Here new algorithms are introduced that allows us to start reorientation right after the separation from the launch vehicle.

In this paper we consider the most common way of attitude control of a spinning satellite. The method is based on the interaction between the geomagnetic field and satellite magnetized elements. Magnetic attitude control systems (MACS) are especially attractive when it is critical to get low-cost and low-mass ACS capable of implementing conventional algorithms for onboard computer. Principal methods of magnetic attitude control of a spinning satellite are considered in [2] and [3]. Paper [4] is a comprehensive survey of works on satellite orientation and stabilization, steady-state motion stability and external torques effect including these problems for a spinning satellite.

1. Problem description

Angular motion of a spinning satellite equipped with MACS is considered in the paper. MACS consists of three mutually orthogonal magnetic coils. Assume that MACS is capable of producing magnetic dipole moment in arbitrary direction in the satellite reference frame but of bounded value. Only torque produced by the interaction of MACS with the geomagnetic field is taken into account. *Averaged geomagnetic field model* is used to represent the geomagnetic field [5]. Angular

motion of a satellite is described by the Beletsky-Chernousko variables [6] and the Euler equations. Satellite's orbit is considered as a Keplerian circular one. MACS implements following algorithms:

1. Nutation damping. Single coil implementing *"-Bdot"* [7] algorithm is used. In some cases general *"-Bdot"* itself may be used.
2. Coarse axis of symmetry reorientation. Two different algorithms are used.
3. Spinning of the satellite around its axis of symmetry. We assume that initial equatorial component of the satellite angular velocity is small due to nutation damping or *"-Bdot"* implementation.
4. Fine axis reorientation in the inertial space. The satellite is assumed to be spinned fast around the axis of symmetry. Two different algorithms are used.

The terminal attitude is the axis of symmetry sun pointing.

2. Geomagnetic field model

The choice of geomagnetic field model is one of the most crucial points for the success of whole work. The most common *inclined dipole model* or *right dipole model* both do not allow us to get the solution of the equations of motions in terms of explicit formulas or quadratures. So, we introduce one more simplification considering the geomagnetic induction vector as moving uniformly on the circular cone side and its magnitude is constant. To do this we need to introduce a reference frame $O_aY_1Y_2Y_3$ where O_a is the Earth center, O_aY_3 axis is directed along the Earth spin axis, O_aY_1 lies in the Earth equatorial plane and is directed to the ascending node, O_aY_2 axis is directed so the system to be a right-handed. If the magnetic induction vector source point is translated to the O_a then the cone is tangent to the O_aY_3 axis, its axis lies in the $O_aY_2Y_3$ plane (figure 1). The cone half-opening angle is given [5] by

$$\mathrm{tg}\,\Theta = \frac{3\sin 2i}{2\left(1-3\sin^2 i+\sqrt{1+3\sin^2 i}\right)} \qquad (2.1)$$

where i is the orbit inclination. The geomagnetic induction vector moves uniformly on the cone side with the double orbital angular speed, $\chi = 2u + \chi_0$ where u is the argument of latitude, ω_0 is the orbital angular velocity. Without loss of generality we can assume $\chi_0 = 0$.

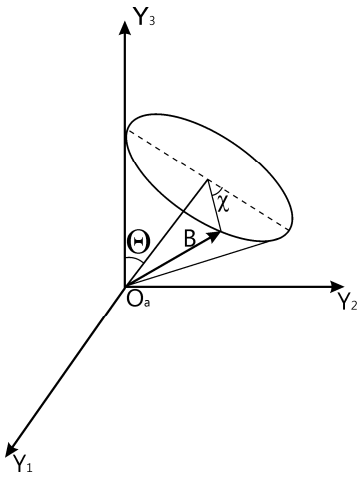

Fig.1. Averaged geomagnetic field model

This model, sometimes called *averaged*, is used in our work. It does not allow us to take into account non-uniformity of geomagnetic induction vector motion (as right dipole model does) and its diurnal change (as inclined dipole model does) but it is considered as a good trade-off between the accuracy of modeling geomagnetic field and the possibility to get closed-form result.

Angle Θ is of great importance for our work. Expression (2.1) introduces the relationship between Θ and the orbit inclination. In fact, these angles are close, so we may consider $\Theta \approx i$ for a qualitative analysis of the system time-response with respect to the orbit inclination since the maximum value of $\Theta - i$ is about 10°. Comprehensive comparison of models can be found in [8].

3. Problem statement

Let us introduce all necessary reference frames.

$O_aZ_1Z_2Z_3$ is the inertial frame, got from $O_aY_1Y_2Y_3$ turning by angle Θ about O_aY_1 axis.

$OL_1L_2L_3$ is the frame associated with the angular momentum of a satellite. O is the satellite's center of mass, OL_3 axis is directed along the angular momentum, OL_2 axis is perpendicular to OL_3 and lies in a plane parallel to the $O_aZ_1Z_2$ plane and containing O, OL_1 is directed such that the reference frame is right-handed.

$Ox_1x_2x_3$ is the bound frame, its axes are directed along the principal axes of inertia of the satellite.

Reference frames mutual orientation is described through the direct cosine matrices $\mathbf{Q}, \mathbf{A}$ expressed in the following tables

	L_1	L_2	L_3
Z_1	q_{11}	q_{12}	q_{13}
Z_2	q_{21}	q_{22}	q_{23}
Z_3	q_{31}	q_{32}	q_{33}

,

	x_1	x_2	x_3
L_1	a_{11}	a_{12}	a_{13}
L_2	a_{21}	a_{22}	a_{23}
L_3	a_{31}	a_{32}	a_{33}

.

We introduce low indices Z, L, x to denote the vector components in frames $O_aZ_1Z_2Z_3$, $OL_1L_2L_3$ and $Ox_1x_2x_3$ respectively. For example, for the first component of a torque in these frames we write M_{1Z}, M_{1L}, M_{1x}.

We use the Beletsky-Chernousko variables and Euler angles to represent the motion of the satellite. Beletsky-Chernousko variables are $L, \rho, \sigma, \varphi, \psi, \theta$ [6] where L is the angular momentum magnitude, angles ρ, σ represent its orientation with respect to $O_aZ_1Z_2Z_3$ frame (figure 2). Orientation of the frame $Ox_1x_2x_3$ with respect to $OL_1L_2L_3$ is described using Euler angles φ, ψ, θ. Direct cosine matrix $\mathbf{Q}$ takes form

$$\mathbf{Q} = \begin{pmatrix} \cos\rho\cos\sigma & -\sin\sigma & \sin\rho\cos\sigma \\ \cos\rho\sin\sigma & \cos\sigma & \sin\rho\sin\sigma \\ -\sin\rho & 0 & \cos\rho \end{pmatrix}. \qquad (3.1)$$

Direct cosine matrix $\mathbf{A}$ is as following

$$\mathbf{A} = \begin{pmatrix} \cos\varphi\cos\psi - \cos\theta\sin\varphi\sin\psi & -\sin\varphi\cos\psi - \cos\theta\cos\varphi\sin\psi & \sin\theta\sin\psi \\ \cos\varphi\sin\psi + \cos\theta\sin\varphi\cos\psi & -\sin\varphi\sin\psi + \cos\theta\cos\varphi\cos\psi & -\sin\theta\cos\psi \\ \sin\theta\sin\varphi & \sin\theta\cos\varphi & \cos\theta \end{pmatrix}. \qquad (3.2)$$

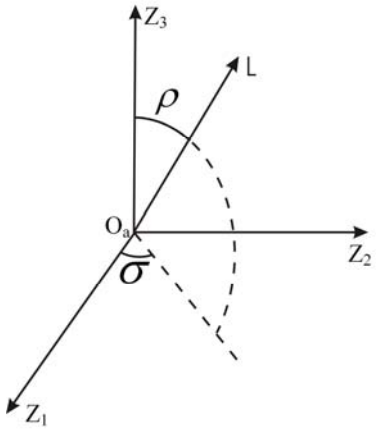

Fig. 2. Angular momentum orientation in the inertial space

Inertia tensor of the satellite is $\mathbf{J}_x = diag(A, A, C)$. Angular motion of the satellite in a circular Keplerian orbit is described [6] by the equations

$$\frac{dL}{dt} = M_{3L},\ \frac{d\rho}{dt} = \frac{1}{L}M_{1L},\ \frac{d\sigma}{dt} = \frac{1}{L\sin\rho}M_{2L},$$

$$\frac{d\theta}{dt} = \frac{1}{L}\left(M_{2L}\cos\psi - M_{1L}\sin\psi\right), \qquad (3.3)$$

$$\frac{d\varphi}{dt} = L\cos\theta\left(\frac{1}{C} - \frac{1}{A}\right) + \frac{1}{L\sin\theta}\left(M_{1L}\cos\psi + M_{2L}\sin\psi\right),$$

$$\frac{d\psi}{dt} = \frac{L}{A} - \frac{1}{L}M_{1L}\cos\psi\,\mathrm{ctg}\,\theta - \frac{1}{L}M_{2L}\left(\mathrm{ctg}\,\rho + \sin\psi\,\mathrm{ctg}\,\theta\right)$$

where M_{1L}, M_{2L}, M_{3L} are the torque components in $OL_1L_2L_3$ frame.

In case of the Euler equations we use variables $\omega_1, \omega_2, \omega_3$ to describe the dynamics of the satellite. In this set ω_i are the components of the absolute angular velocity of the satellite in $Ox_1x_2x_3$ frame ($i = 1,2,3$). Satellite dynamics is described by equations

$$A\frac{d\omega_1}{dt} - (A - C)\omega_2\omega_3 = M_{1x},$$

$$A\frac{d\omega_2}{dt} + (A - C)\omega_1\omega_3 = M_{2x}, \qquad (3.4)$$

$$C\frac{d\omega_3}{dt} = M_{3x},$$

kinematic relations are not used.

4. Initial attitude acquisition

Since small satellites are of particular interest in this work, initial conditions after the separation from the launch vehicle cannot be restricted during mission design period. So, coarse pointing and detumbling are necessary prior to fine pointing algorithm implementation.

4.1. Nutation damping

Algorithm "*-Bdot*" [7] is the most common way for detumbling the satellite at the initial stage of mission. However, in the considered case its implementation may be illogical since the satellite should be spinned about its axis of symmetry, so damping the angular velocity component along the axis of symmetry is undesirable. Instead, nutation damping algorithm is used. It is discussed in another work [1], so we bring only brief analysis here. We will use the "*-Bdot*" algorithm implemented by a single coil only. Magnetic dipole moment of the satellite $\mathbf{m}_x = (0,0,m)^T$ in this case is determined by the expression

$$\mathbf{m}_x = -k_1 \left(\frac{d\mathbf{B}_x}{dt} \mathbf{e}_3 \right) \mathbf{e}_3 , \qquad (4.1)$$

where k_1 is a positive coefficient, $\mathbf{e}_3$ is a unit vector of the axis of symmetry of the satellite.

Consider fast rotations of a satellite ($L / A >> \omega_0$, $L / C >> \omega_0$). Such a regime is typical for the initial rotation of a satellite after the separation from launcher. Our assumption is further justified when one notes that the nutation damping algorithm is the first in sequence and it is implemented right after the separation.

After some mathematics the magnetic dipole moment of the single coil in $OL_1L_2L_3$ frame is

$$m = \frac{L}{A} k_1 \left[B_{1L} \left(a_{31} a_{12} - a_{32} a_{11} \right) + B_{2L} \left(a_{31} a_{22} - a_{32} a_{21} \right) \right]$$

and the dipole moment of the satellite is

$$\mathbf{m}_L = \mathbf{A}\mathbf{m}_x = m \left(a_{13}, \quad a_{23}, \quad a_{33} \right)^T,$$

which leads to the torque

$$\mathbf{M}_L = m \begin{pmatrix} a_{23} B_{3L} - a_{33} B_{2L} \\ a_{33} B_{1L} - a_{13} B_{3L} \\ a_{13} B_{2L} - a_{23} B_{1L} \end{pmatrix}.$$

Let us transform equations of motion to the dimensionless form. These equations will be used for other algorithms analysis with slight revision. In order to do this we use dimensionless torque $\overline{\mathbf{M}}_L$ defined by the expression

$$\mathbf{M}_L = \frac{k_1 B_0^2 L}{A} \overline{\mathbf{M}}_L. \tag{4.2}$$

Next we introduce argument of latitude $u = \omega_0 (t - t_0)$ instead of time in (3.3) and dimensionless angular momentum l according to the expression $L = L_0 l$ where L_0 is the initial angular momentum magnitude. This leads to (3.3) being rewritten as

$$\begin{aligned}
&\frac{dl}{du} = \varepsilon l \overline{M}_{3L}, \frac{d\rho}{du} = \varepsilon \overline{M}_{1L}, \frac{d\sigma}{du} = \frac{\varepsilon}{\sin\rho} \overline{M}_{2L}, \\
&\frac{d\theta}{du} = \varepsilon \left(\overline{M}_{2L} \cos\psi - \overline{M}_{1L} \sin\psi \right), \\
&\frac{d\varphi}{du} = \eta_1 l \cos\theta + \frac{\varepsilon}{\sin\theta} \left(\overline{M}_{1L} \cos\psi + \overline{M}_{2L} \sin\psi \right), \\
&\frac{d\psi}{du} = \eta_2 l - \varepsilon \overline{M}_{1L} \cos\psi \operatorname{ctg}\theta - \varepsilon \overline{M}_{2L} \left(\operatorname{ctg}\rho + \sin\psi \operatorname{ctg}\theta \right).
\end{aligned} \tag{4.3}$$

The following notations $\varepsilon = \frac{k_1 B_0^2}{\omega_0 A}$, $\eta_1 = \frac{L_0}{\omega_0}\left(\frac{1}{C} - \frac{1}{A}\right)$, $\eta_2 = \frac{L_0}{A\omega_0}$ are introduced. In case of weak magnetic dipole moment ε and expressions $\frac{\varepsilon}{\eta_i} \sim \frac{k_1 B_0^2}{L_0}$ are small. Parameter ε can be regarded as the ratio between angular momentum change during one orbit and its mean value on this interval; $\frac{\varepsilon}{\eta_i}$ are the same but for one satellite's revolution about its center of mass. It is seen from (4.3) that φ, ψ, u are fast variables, while l, ρ, σ, θ are slow ones. So, we can use asymptotical methods [9] to determine slow variables evolution. In order to do that we need to average equations along the undisturbed solution of equations (4.3). However, since this motion is a regular precession, we need only to average separately the equations for slow variables over fast variables. Equations (4.3) and following reasoning will be used again for other algorithms.

For the nutation damping algorithm we get on the time interval of order $1/\varepsilon$

$$\begin{aligned}
&\frac{dl}{du} = -\frac{1}{2}\varepsilon l\left[2p + (1-3p)\sin^2\rho\right]\sin^2\theta, \\
&\frac{d\rho}{du} = \frac{1}{2}\varepsilon(3p-1)\sin\rho\cos\rho\sin^2\theta, \\
&\frac{d\theta}{du} = -\frac{1}{2}\varepsilon\left[2p + (1-3p)\sin^2\rho\right]\sin\theta\cos\theta, \\
&\frac{d\sigma}{du} = 0
\end{aligned} \qquad (4.4)$$

where $p = 0.5\sin^2\Theta$. Equations (4.4) admit two first integrals. The first one is $I_1(l,\theta) = l\cos\theta$. It shows that the third component of angular velocity vector conserves in the fixed frame. Another first integral is $I_2(\rho,\theta) = \frac{1}{2}\ln\left(\mathrm{tg}^2\rho + 1\right) - \frac{2p}{3p-1}\ln\mathrm{tg}\rho + \ln\cos\theta$.

We got two first integrals satisfying conditions of the implicit function theorem so the solution of (4.4) is obtained in quadratures.

There are three parameters which affect the time-response: i, ρ_0, θ_0. As expected, with θ_0 rise the time response (the time necessary to lower θ, and, therefore, the equatorial component of angular velocity $l \sin\theta / A$) falls. Parameter i and ρ_0 effect is presented in figures 3 and 4.

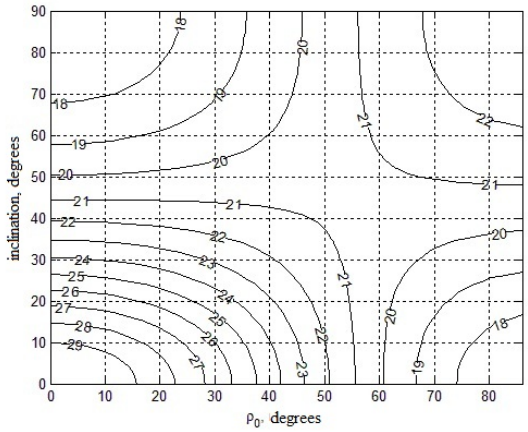

Fig. 3. Angle θ after 2 orbits, $\theta_0 = 30^\circ$

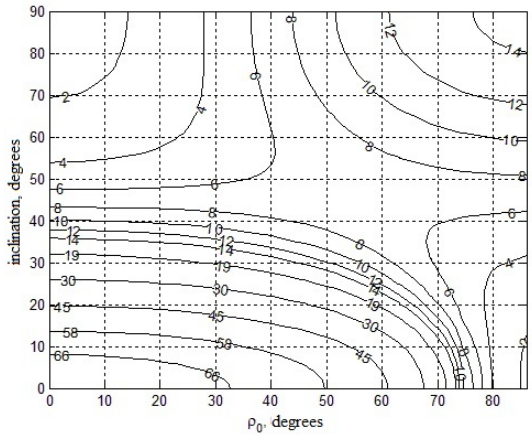

Fig. 4. Angle θ after 15 orbits, $\theta_0 = 70^\circ$

As seen from figure 2, if ρ_0 is less than approximately 50° the time response rises with inclination rise, and if ρ_0 is greater, it falls. Figure 3 shows that if the algorithm is considered on greater time interval, there is some area where the best inclination is about 45°. But it is clear that for the greater inclination θ would not exceed 14°, while for the small inclination it may stay almost constant. So, it is preferable to use high-inclined orbit.

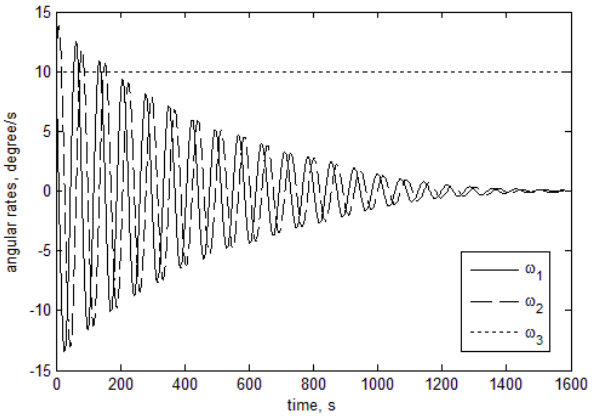

Fig. 5. Numerical simulation

Figure 5 brings numerical simulation of the nutation damping algorithm performance. Numerical analysis was conducted under following assumptions:

- Satellite tensor of inertia is $\mathbf{J} = diag\left(0.2, 0.2, 0.3\right) kg \cdot m^2$
- The gain $k_1 = 2 \cdot 10^6 kg \cdot m^2 / T^2 \cdot s$
- Initial angular velocity of the satellite is $\left(10, 10, 10\right)^T$ deg/ s
- Orbit inclination is 60°
- Orbit altitude is 400 km
- IGRF model is used (for the orbit with 400 km altitude).

Apart of initial conditions, other parameters will be used in further numerical simulations. It is seen from figure 5 that the algorithm effectively damps nutational motion.

4.2. First coarse reorientation algorithm

One way to achieve a terminal orientation is successive implementation of nutation damping, spinning and reorientation algorithm. However, one can start reorientation right after the separation from the launch vehicle. Coarse sun-pointing algorithm is used [10]

$$\mathbf{m} = k_2 \left(\mathbf{e}_3 \left[\mathbf{B} \times \mathbf{S} \right] \right) \mathbf{e}_3 . \qquad (4.5)$$

The analysis of the satellite motion with this algorithm implemented is rather complex, so we consider one special case $\mathbf{S}_Z = \left(0, 0, 1\right)^T$. That means the Sun pointing vector is directed along the axis of the cone in the averaged geomagnetic field model. Satellite is considered as fast rotating again since the coarse algorithm is used right after the separation. So, we use equations (4.3) and all related reasoning to get averaged equations. We need the torque to be written in $OL_1L_2L_3$ frame. Sun-pointing vector is $\mathbf{S}_L = \left(q_{31}, 0, q_{33}\right)^T$ since $q_{32} = 0$. Geomagnetic induction vector is

$$\mathbf{B}_L = \begin{pmatrix} q_{11}B_{1Z} + q_{21}B_{2Z} + q_{31}B_{3Z} \\ q_{12}B_{1Z} + q_{22}B_{2Z} + q_{32}B_{3Z} \\ q_{13}B_{1Z} + q_{23}B_{2Z} + q_{33}B_{3Z} \end{pmatrix},$$

axis of symmetry is

$\mathbf{e}_{3L} = (a_{31}, a_{32}, a_{33})$.

We introduce vector $\mathbf{p} = \mathbf{B} \times \mathbf{S}$ for simplicity. The torque is

$$\mathbf{M}_L = k_2 B_0^2 \begin{pmatrix} p_1 B_{3Z} a_{13} a_{23} + p_2 B_{3Z} a_{23}^2 + p_3 B_{3Z} a_{33} a_{323} - p_1 B_{2Z} a_{13} a_{33} - p_2 B_{2Z} a_{23} a_{33} - p_3 B_{2Z} a_{33}^2 \\ p_1 B_{1Z} a_{13} a_{33} + p_3 B_{1Z} a_{33}^2 + p_2 B_{1Z} a_{33} a_{23} - p_2 B_{3Z} a_{13} a_{23} - p_3 B_{3Z} a_{13} a_{33} - p_1 B_{3Z} a_{13}^2 \\ p_2 B_{2Z} a_{13} a_{23} + p_1 B_{2Z} a_{13}^2 + p_3 B_{2Z} a_{33} a_{13} - p_1 B_{1Z} a_{13} a_{23} - p_3 B_{1Z} a_{23} a_{33} - p_2 B_{1Z} a_{23}^2 \end{pmatrix} \quad (4.6)$$

In order to derive equations for slow variables, we need to obtain expressions for $\langle M_{iL} \rangle_{\varphi,\psi,u}, \langle M_{1L} \cos\psi \rangle_{\varphi,\psi,u}, \langle M_{2L} \sin\psi \rangle_{\varphi,\psi,u}$. Components M_{iL} do not contain φ. Only expressions $a_{ij}a_{kl}$ contain ψ, while expressions $B_i B_j$ contain u. So, only $a_{ij}a_{kl}$ should be averaged over ψ, and only $B_i B_j$ should be averaged over u. The latter leads to $B_{11} = B_{22} = 0.5\sin^2\Theta = p$, $B_{33} = \cos^2\Theta = q$. Averaging leads to equations

$$\begin{aligned} \frac{dl}{du} &= \varepsilon p \sin^2\theta \cos\rho, \\ \frac{d\rho}{du} &= \varepsilon p \left(0.5\sin^2\theta - 1\right)\sin\rho / l, \\ \frac{d\sigma}{du} &= 0, \\ \frac{d\theta}{du} &= \varepsilon p \sin\theta \cos\theta \cos\rho / l \end{aligned} \quad (4.7)$$

where $\varepsilon = \dfrac{k_2 B_0^2}{L_0 \omega_0}$. New small parameter has the same sense. It is introduced because damping coefficients in algorithms are different. The same notation ε is used for convenience for the analysis of each algorithm. We immediately obtain the first integral $\sigma = const$ (trivial equation for σ is omitted from now on). Next, we divide the first equation in (4.7) with the last one,

$$\frac{dl}{l}=\frac{\sin\theta}{\cos\theta}d\theta.$$

That leads to the important first integral $I_1(l,\theta)=l\cos\theta$. It means that the spinning rate, that is, ω_3 does not change during the coarse reorientation process. It eliminates the danger of satellite being spinned too fast or detumbled. However, we have no insight on the precession rate. In order to obtain second first integral we divide second equation in (4.7) with the last one,

$$\frac{d\rho}{d\theta}=\frac{\sin\rho}{\cos\rho}\frac{0.5\sin^2\theta-1}{\sin\theta\cos\theta}.$$

That leads to the integral

$$I_2(\rho,\theta)=0.25\ln\left(\mathrm{tg}^2\theta+1\right)-\ln\mathrm{tg}\,\theta-\ln\sin\rho.$$

These two first integrals bring the solution of (4.7) in quadratures.

Equations (4.7) have two equilibrium points $(\theta=0,\ \rho=0 \text{ or } \pi)$ and $(\theta=\pi/2,\ \rho=0 \text{ or } \pi)$, the first equation is separated. Only the point $(\theta=\pi/2,\ \rho=0)$ is stable, so angle ρ tends to zero. Angular momentum magnitude and nutation rate rise. In order to interpret this result, let us analyze the control law (4.5). Clearly, it forces the satellite to one of two positions: $[\mathbf{e}_3\times\mathbf{B}]=0$, that is geomagnetic attitude of the axis of symmetry, or $\mathbf{e}_3[\mathbf{B}\times\mathbf{S}]=0$, that is the axis of symmetry lying in the plane of vectors $\mathbf{B},\mathbf{S}$. Position $[\mathbf{e}_3\times\mathbf{B}]=0$ is only the special case of axis of symmetry lying in the plane $(\mathbf{B},\mathbf{S})$. In our special case vector $\mathbf{S}$ coincides with the axis of the cone in averaged geomagnetic field model. After averaging the motion over fast angles φ and ψ the axis of symmetry coincides with the angular momentum vector. So, vector $\mathbf{L}$ should rotate with the plane $(\mathbf{B},\mathbf{S})$. After the motion is averaged over one orbit, angular momentum vector eventually coincides with the axis of the cone which is represented by angle ρ tending to zero. So, the time necessary for angle ρ to become zero may be considered as time-

response of the algorithm (4.5). The time-response is affected by inclination (since p depends on Θ and, therefore, on i) and θ_0. Figure 6 makes their influence clear.

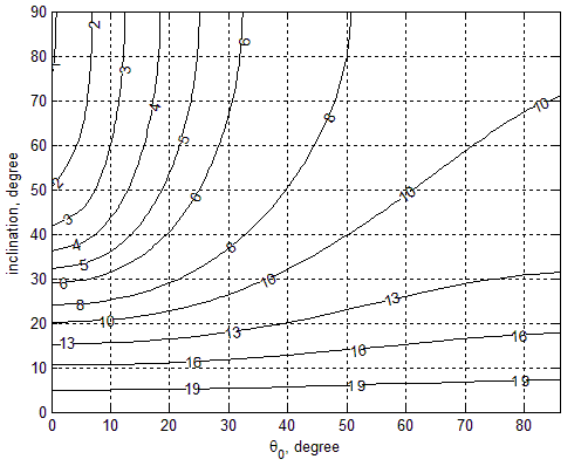

Fig. 6. Angle ρ after 10 orbits, $\rho_0 = 20^\circ$

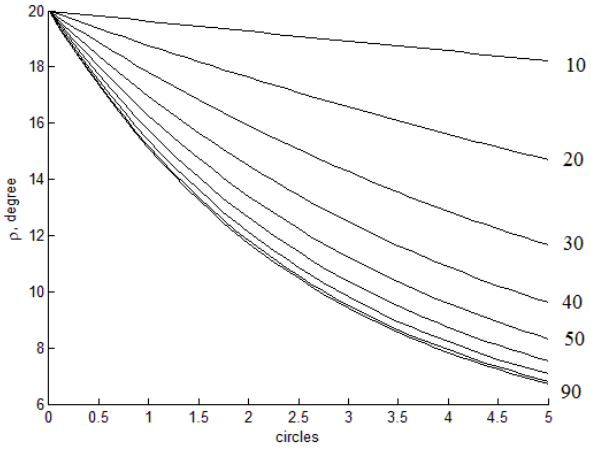

Fig. 7. Angle ρ for a set of inclinations

Figure 6 brings angle ρ after 10 circles for different inclinations and θ_0 values. It is seen that θ_0 effects the time-response and it is better to have it small (that means to have satellite possibly close to being spin-stabilized). So, the closer the satellite to the spinning around the axis of symmetry, the better. Inclination has dramatic effect on time-response. It is clearly better to have high inclinations: for inclinations less than 10° ρ keeps almost constant (changes by several degrees), while for high inclinations it reduces to only few degree. Figure 7 introduces angle ρ with respect to time for different inclinations and $\theta_0 = 20^\circ$.

The attitude of the axis of symmetry lying in the plane $(\mathbf{B},\mathbf{S})$ is not exactly the desired. In order to achieve sun-pointing, nutation damping (4.1) is introduced. It does not change the spinning, since $l\cos\theta$ is the first integral for both algorithms but it decreases nutation that arises with algorithm (4.5) (since l rises and θ tends to zero). In terms of axis of symmetry lying in the plane $(\mathbf{B},\mathbf{S})$ it also decreases angular velocity that arises because of rotating vector $\mathbf{B}$. So, the axis of symmetry slowly tends to coincide with $\mathbf{S}$. However, when coarse attitude is achieved and nutation is damped, it is logical to switch to the spinning algorithm and then to the fine sun-

pointing one. Figures 8-10 introduce numerical analysis of combined implementation of algorithms (4.1) and (4.5).

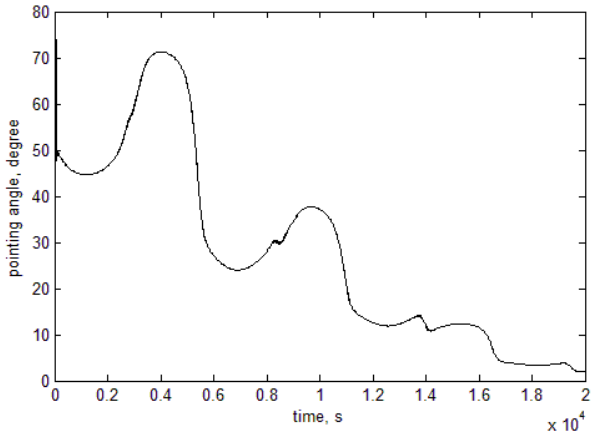

Fig. 8. Pointing angle evolution.

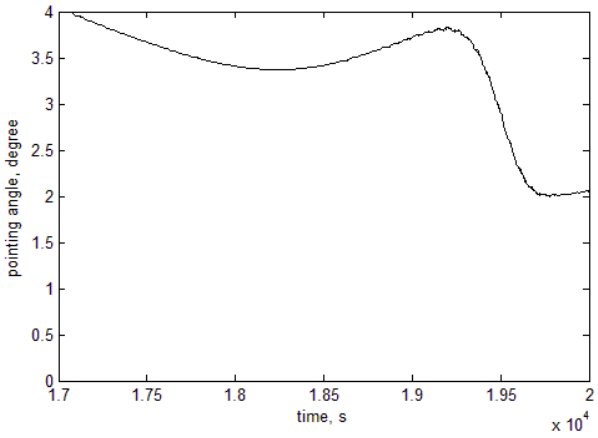

Fig. 9. Final pointing accuracy.

Figures 8 and 9 bring the pointing accuracy of the first coarse reorientation algorithm (simulation time is about 4 circles). The accuracy is about two degree, which is good for the coarse sun-pointing. It is possible to achieve even better accuracy with different initial conditions but generally the accuracy is about few degree.

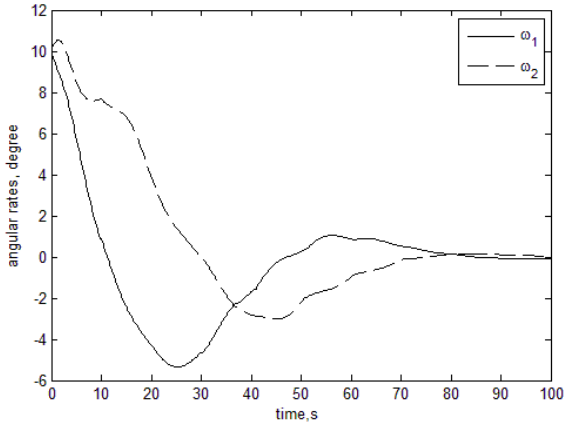

Fig. 10. Angular velocity rate

Figure 10 shows nutation damping when implementing both coarse reorientation algorithm and nutation damping. Simulations were held with following initial conditions:

- Initial Euler angles are $\alpha = \alpha_s - 10°$, $\beta = \beta_s + 7°$, $\gamma = \gamma_s - 61.3°$
- Initial pointing error is 12˚

- Angular rates $\omega_x = \omega_y = \omega_z = 10° / \mathrm{s}$
- Damping and reorientation gains are $k_1 = 5 \cdot 10^6 kg \cdot m^2 / T^2 \cdot s$, $k_2 = 10^6 kg \cdot m^2 / T^2 \cdot s^2$.

Orbit inclination and geomagnetic field model here and further are the same as for the nutation damping numerical analysis. Angles $\alpha_s, \beta_s, \gamma_s$ meaning is briefly described below. We introduce new Sun-related reference frame $O_a S_1 S_2 S_3$ where $O_a S_3$ coincides with the Sun direction, $O_a S_1$ axis is directed as the cross product of $O_a Z_3$ and $O_a S_3$, while $O_a S_2$ is directed such that the reference frame is right-handed. When the body frame $Ox_1x_2x_3$ coincides with the $O_a S_1 S_2 S_3$ frame the satellite is actually pointing at the Sun. The new set of Euler angles $\alpha_s, \beta_s, \gamma_s$ is used to describe $Ox_1x_2x_3$ attitude relative to $O_a S_1 S_2 S_3$. So the initial attitude is represented as a deviation from a perfect Sun pointing.

4.3. Second coarse reorientation algorithm

Paper [1] introduces fine reorientation algorithm implemented by the third coil

$$\mathbf{m} = k_3 \left(0,\, 0,\, \left(\mathbf{S} - \mathbf{L}\right)\left[\mathbf{e}_3 \times \mathbf{B}\right]\right). \qquad (4.8)$$

This algorithm is used for the spinned satellite when the axis of symmetry coincides with the angular momentum. So, it may be rewritten in the form

$$\mathbf{m} \approx k_3 \left(0,\, 0,\, \left(\mathbf{S} - \mathbf{e}_3\right)\left[\mathbf{e}_3 \times \mathbf{B}\right]\right).$$

Taking into account $\mathbf{e}_3\left[\mathbf{e}_3 \times \mathbf{B}\right] = 0$ it becomes identical to (4.5). The analysis of the algorithm (4.8) for the case of already spinned satellite can be found in [1] and is briefly considered in section 6. Here we try to use it for the coarse reorientation in the case of arbitrary initial angular velocity. Magnetic dipole moment of the third coil is

$$m_3 = k_3 B_0 \left[S_1 \left(a_{23} B_3 - a_{33} B_2\right) + \left(S_3 - 1\right)\left(a_{13} B_2 - a_{23} B_1\right)\right]$$

where S_i are components of the direction to the Sun vector in $OL_1L_2L_3$ frame (we consider $\mathbf{S}_Z = (0, 0, 1)^T$ again). The torque is

$$\mathbf{M}=k_3B_0^2\begin{pmatrix} S_1\left(a_{23}^2B_3^2-2a_{23}a_{33}B_2B_3+a_{33}^2B_2^2\right)+\left(S_3-1\right)\left(a_{23}a_{13}B_2B_3-a_{23}^2B_1B_3+a_{23}a_{33}B_2B_1-a_{33}a_{13}B_2^2\right) \\ S_1\left(a_{23}a_{33}B_1B_3-a_{33}^2B_1B_2+a_{13}a_{33}B_2B_3-a_{23}a_{13}B_3^2\right)+\left(S_3-1\right)\left(a_{33}a_{13}B_2B_1-a_{13}^2B_2B_3+a_{13}a_{23}B_3B_1-a_{33}a_{23}B_1^2\right) \\ S_1\left(a_{23}a_{13}B_2B_3-a_{23}^2B_1B_3+a_{23}a_{33}B_2B_1-a_{33}a_{13}B_2^2\right)+\left(S_3-1\right)\left(a_{13}^2B_2^2-2a_{23}a_{13}B_2B_1+a_{23}^2B_1^2\right) \end{pmatrix}.$$

It does not depend on φ again, and we need to average expressions $a_{ij}a_{kl}$ over ψ and expressions B_iB_j over u. Averaged equations are

$$\begin{aligned} \frac{dl}{du} &= \frac{1}{2}\varepsilon\sin^2\theta\left[2p\left(\cos\rho-1\right)+\left(3p-1\right)\sin^2\rho\right], \\ \frac{d\rho}{du} &= -\varepsilon p\sin\rho/l+\frac{1}{2}\varepsilon\sin^2\theta\left[p\sin\rho+\left(3p-1\right)\sin\rho\cos\rho\right]/l, \\ \frac{d\sigma}{du} &= 0, \\ \frac{d\theta}{du} &= \frac{1}{2}\varepsilon\sin\theta\cos\theta\left[2p\left(\cos\rho-1\right)+\left(3p-1\right)\sin^2\rho\right]/l. \end{aligned} \tag{4.9}$$

where $\varepsilon=\dfrac{k_3B_0^2}{\omega_0}$. These equations admit first integral $I_1(l,\theta)=l\cos\theta$. Unfortunately, no other first integrals can be obtained. Nevertheless equations (4.9) are proper for numerical integration since they do not contain equations for variables with different change rates. The first integral may be used to control the accuracy of numerical integration. The time-response is determined by the time necessary for the angle ρ to become close to zero again. Figures 11 and 12 introduce this angle for different inclinations and initial values of angle θ.

The time is 10 orbits and $\rho_0 = 20^\circ$ again, so we can compare two coarse sun-pointing algorithms. Clearly, if $\theta_0 > 45^\circ$ low inclination is better. All other algorithms act better for high inclinations, so we consider this case. If the inclination is high, θ_0 should be less than 45°. However, for $\theta_0 < 45^\circ$ the time-response is better than for the

algorithm (4.5). So, for the best time-response it is logical to implement algorithm (4.5) along with the nutation damping algorithm, and when θ becomes less than 45° to switch to the algorithm (4.8). It is not necessary to terminate nutation damping algorithm though. The algorithm (4.8) does not increase the nutation rate. Figure 8 introduces angle θ starting from $\theta_0 = 40^\circ$ (that means algorithm (4.8) is already implemented instead of initial (4.5)). It is seen that for high inclinations we may neglect the nutation damping effect of algorithm (4.8). If the inclination is low this algorithm becomes especially important. It provides relatively fast coarse reorientation in case of large initial nutation rate and detumbles the satellite keeping the spinning rate. However, this is valid only if satellite angular momentum initial attitude is far from necessary (ρ is not small).

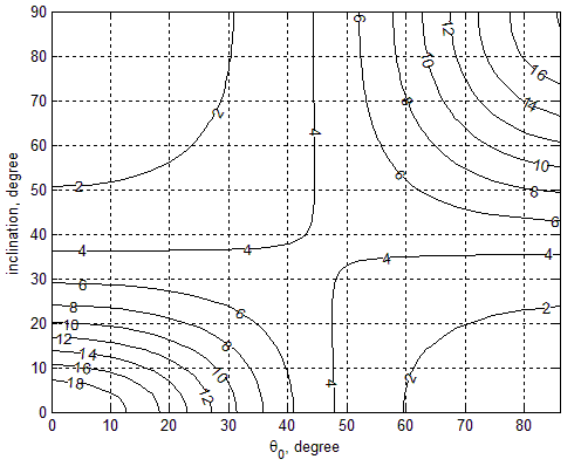

Fig. 11. Angle ρ after 10 orbits, $\rho_0 = 20^\circ$

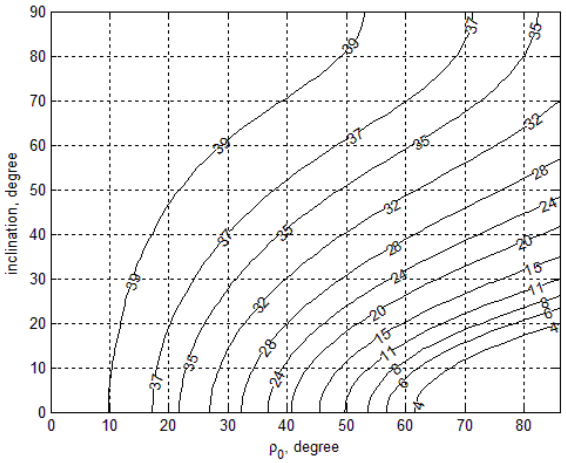

Fig. 12. Angle θ after 10 orbits, $\theta_0 = 40^\circ$

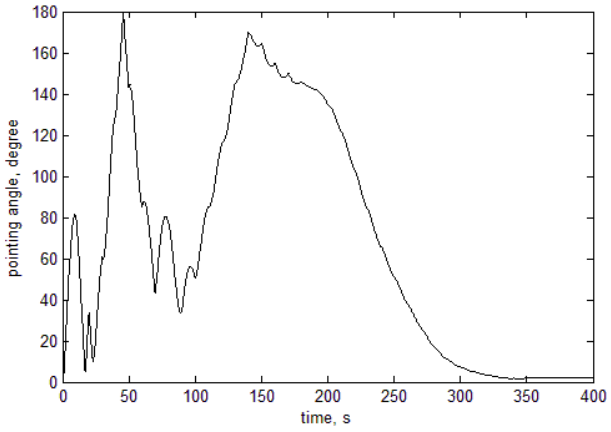

Fig. 13. Pointing angle evolution.

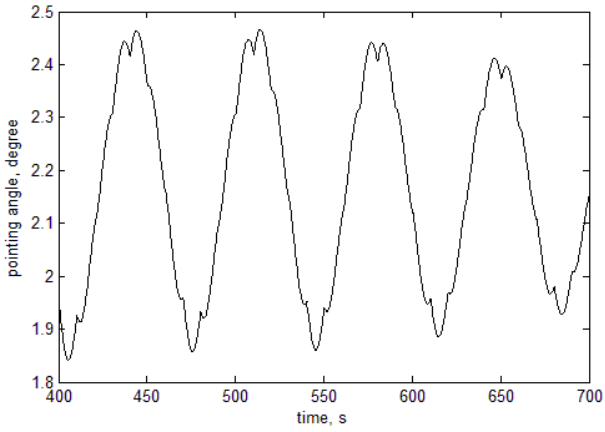

Fig. 14. Final pointing accuracy.

Figures 13-15 introduce numerical analysis of combined implementation of algorithms (4.1) and (4.8) for a chaotically rotating satellite. Figures 13 and 14 bring the pointing accuracy of the second coarse reorientation algorithm. The accuracy is about 3 degree, which is proper for the coarse sun-pointing. It is possible to achieve even better accuracy with different initial conditions but generally the accuracy is about few degree.

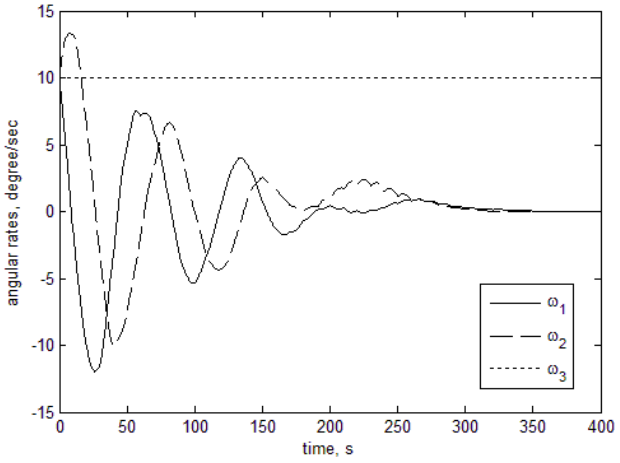

Fig. 15. Angular velocity rate

Figure 15 shows nutation damping when implementing both coarse reorientation algorithm and nutation damping. The following set of initial conditions have been used:

- Initial Euler angles are $\alpha = \alpha_s + 12.6°$, $\beta = \beta_s - 16°$, $\gamma = \gamma_s - 61.3°$
- Initial pointing error is 19.6°
- Angular rates $\omega_x = \omega_y = \omega_z = 10° / \mathrm{s}$
- Damping and reorientation gains are $k_1 = 5 \cdot 10^7 kg \cdot m^2 / T \cdot s$, $k_2 = 10^6 kg \cdot m^2 / T \cdot s^2$.

If the satellite is already spinned the results are better. Figure 16 introduces the pointing accuracy for this case.

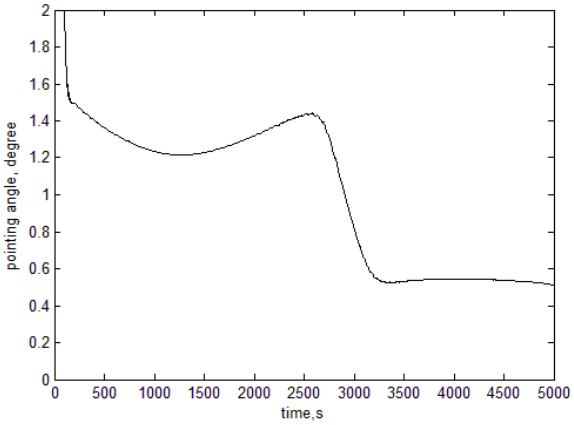

Fig. 16. Pointing angle evolution

The following set of initial conditions have been used:

- Initial Euler angles are $\alpha = \alpha_s - 10°$, $\beta = \beta_s + 7°$, $\gamma = \gamma_s - 61.3°$
- Initial pointing error is 12˚
- Angular rates $\omega_x = \omega_y = 0$, $\omega_z = 10° / s$
- Damping reorientation gains are $k_1 = 5 \cdot 10^7 kg \cdot m^2 / T \cdot s$, $k_2 = 10^6 kg \cdot m^2 / T \cdot s^2$

5. Spinning up

It is shown in previous section that initial attitude acquisition phase leads to the satellite being reoriented in the necessary direction (by means of algorithms (4.5) and/or (4.8)) with damped nutation rate (by means of algorithms (4.1) and/or (4.8)). Spinning rate is not affected at all. In order to achieve the spin stabilization the satellite should be spinned around the axis of symmetry to the proper angular velocity ω_f. This is achieved with the algorithm

$$\mathbf{m}_x = k_4 \left(B_{2x}, -B_{1x}, 0 \right)^T \qquad (5.1)$$

leading to the torque

$$\mathbf{M}_x = k_4 B_0^2 \left(-B_{1x} B_{3x}, -B_{2x} B_{3x}, B_{1x}^2 + B_{2x}^2 \right). \qquad (5.2)$$

5.1. Model problem

We use Euler equations (3.4). Clearly, if we consider the torque (5.2), M_{3x} is always positive. We substitute M_{3x} with positive constant value as well as M_{1x} and M_{2x} ones but with less values since the actual sign of these components changes and by substituting them with positive constant values we only worsen the situation. We also consider satellite nutation as being damped after the initial attitude acquisition stage. So, we analyze equations

$$A\frac{d\omega_1}{dt}-(A-C)\omega_2\omega_3=M_1,$$

$$A\frac{d\omega_2}{dt}+(A-C)\omega_1\omega_3=M_2, \qquad (5.3)$$

$$C\frac{d\omega_3}{dt}=M_3$$

Assume the initial angular velocity in this stage $\boldsymbol{\omega}_0=(\omega_{10},\omega_{20},\omega_{30})^T$ is no equal to zero but either all of its components are small in comparison with ω_f or only equatorial component is small. For the further analysis we only need $\omega_{i0}/\omega_f=o(1)$, $(i=1,2)$ which means that the initial equatorial component is small. The component M_3 along the axis of symmetry is the prevailing one, i.e. $|M_1|<<|M_3|$, $|M_2|<<|M_3|$. This should lead to the spinning around the axis of symmetry.

The latter equation in (5.3) is instantly solved

$$\omega_3=\omega_{30}+\frac{M_3}{C}t$$

and this expression leads to the time $t_{rot}=\frac{C}{M_3}\left(\omega_f-\omega_{30}\right)$ necessary to achieve the required velocity ω_f.

To get two first components of angular velocity we introduce a new time

$$\tau=\frac{C}{2M_3}\left(\omega_{30}+\frac{M_3}{C}t\right)^2$$

and denote $a=\frac{M_1}{A}\sqrt{\frac{C}{2M_3}}$, $b=\frac{M_2}{A}\sqrt{\frac{C}{2M_3}}$. Then (5.3) take a form

$$\frac{d\omega_1}{d\tau}-\lambda\omega_2=\frac{a}{\sqrt{\tau}},\ \frac{d\omega_2}{d\tau}+\lambda\omega_1=\frac{b}{\sqrt{\tau}}$$

where $\lambda=\frac{A-C}{A}$. Homogenous equations solution is as following

$$\omega_1=c_1\cos\lambda\tau+c_2\sin\lambda\tau,\ \omega_2=-c_1\sin\lambda\tau+c_2\cos\lambda\tau.$$

Varying constants $c_1,\ c_2$ we get the following equations

$$\frac{dc_1}{d\tau}=a\frac{\cos\lambda\tau}{\sqrt{\tau}}-b\frac{\sin\lambda\tau}{\sqrt{\tau}},\ \frac{dc_2}{d\tau}=a\frac{\sin\lambda\tau}{\sqrt{\tau}}+b\frac{\cos\lambda\tau}{\sqrt{\tau}}$$

with a solution

$$c_1=a\sqrt{\frac{2\pi}{\lambda}}C(\lambda\tau)-b\sqrt{\frac{2\pi}{\lambda}}S(\lambda\tau)+c_{10},$$

$$c_2=a\sqrt{\frac{2\pi}{\lambda}}S(\lambda\tau)+b\sqrt{\frac{2\pi}{\lambda}}C(\lambda\tau)+c_{20}$$

where $C(x)=\frac{1}{\sqrt{2\pi}}\int_0^x\frac{\sin y}{\sqrt{y}}dy$, $S(x)=\frac{1}{\sqrt{2\pi}}\int_0^x\frac{\cos y}{\sqrt{y}}dy$ are the Fresnels integrals [11], c_{10}, c_{20} are constants of integration. Note, that the Fresnels integrals are odd functions. So, if $\lambda<0$ then $S(\lambda\tau)=-S(|\lambda|\tau), C(\lambda\tau)=-C(|\lambda|\tau)$. The sign of λ has no impact on the further argument. We denote

$$c'=a\sqrt{\frac{2\pi}{\lambda}}C(\lambda\tau)-b\sqrt{\frac{2\pi}{\lambda}}S(\lambda\tau),\ c''=a\sqrt{\frac{2\pi}{\lambda}}S(\lambda\tau)+b\sqrt{\frac{2\pi}{\lambda}}C(\lambda\tau),$$

$$c_0'=a\sqrt{\frac{2\pi}{\lambda}}C(\lambda\tau_0)-b\sqrt{\frac{2\pi}{\lambda}}S(\lambda\tau_0),\ c_0''=a\sqrt{\frac{2\pi}{\lambda}}S(\lambda\tau_0)+b\sqrt{\frac{2\pi}{\lambda}}C(\lambda\tau_0).$$

So, using the initial conditions we obtain

$$\omega_{10}=(c_0'+c_{10})\cos\lambda\tau_0+(c_0''+c_{20})\sin\lambda\tau_0,\ \omega_{20}=-(c_0'+c_{10})\sin\lambda\tau_0+(c_0''+c_{20})\cos\lambda\tau_0$$

which leads to

$$c_{10}=(\omega_{10}\cos\lambda\tau_0-\omega_{20}\sin\lambda\tau_0)-c_0',\ c_{20}=(\omega_{10}\sin\lambda\tau_0+\omega_{20}\cos\lambda\tau_0)-c_0''.$$

Since $|\omega_{10}| << |\omega_f|$, $|\omega_{20}| << |\omega_f|$ we need to compare $c' - c_0'$ and $c'' - c_0''$ with ω_f in order to compare ω_1 and ω_2 with ω_f. The Fresnels integrals $C(x)$ and $S(x)$ are less than unity by magnitude, so we need to consider expressions

$$\varepsilon_i = \frac{M_i}{A\omega_f}\sqrt{\frac{C}{2M_3}}, \ (i = 1,2).$$

We have $\varepsilon_i = o(1)$ since the components M_1, M_2 are small in comparison with the component M_3 and $A\omega_f$. So, if initial equatorial component of the angular velocity $\omega_\perp$ is small and the torque is directed almost along the axis of symmetry, conditions $|\omega_1| << |\omega_3|$, $|\omega_2| << |\omega_3|$ are satisfied and the satellite may be considered spinning around the axis of symmetry. Fig. 17 introduces the ratio $\omega_\perp / \omega_3$ with respect to the time.

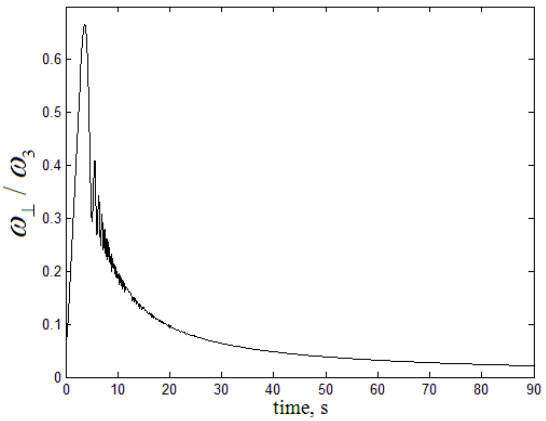

Fig. 17. The ratio between the equatorial and polar components of angular velocity

Equatorial component $\omega_\perp$ is finite and raises with expressions $\frac{M_1}{M_3}$, $\frac{M_2}{M_3}$ rise. It is not damped to zero but to some minimum value which depends on $\frac{M_1}{M_3}$, $\frac{M_2}{M_3}$. In figure 7 the ratio $\frac{M_i}{M_3} = o(1)$, $(i = 1,2)$.

5.2. Real control law

Constant torque cannot be achieved with MACS. Paper [1] introduces analysis of the control law (5.1). Here it is briefly considered. Averaged Beletsky-Chernousko equations in case of small angle θ are as follows

$$\frac{dl}{du} = \varepsilon\left[2p + (1-3p)\sin^2\rho\right],$$

$$\frac{d\rho}{du} = -\varepsilon\frac{1}{l}(3p-1)\sin\rho\cos\rho,$$

$$\frac{d\theta}{du} = -\frac{1}{2l}\varepsilon\left[2-2p-(1-3p)\sin^2\rho\right]\theta$$

where $\varepsilon = \dfrac{k_4 B_0^2}{\omega_0 L_0}$. These equations admit the first integral $I_1(l,\rho) = \ln l - \dfrac{1}{2}\ln\left(\mathrm{tg}^2\rho + 1\right) + \dfrac{2p}{3p-1}\ln\mathrm{tg}\rho$ and equation for θ is separated. Figure 18 bring the time-response of the algorithm.

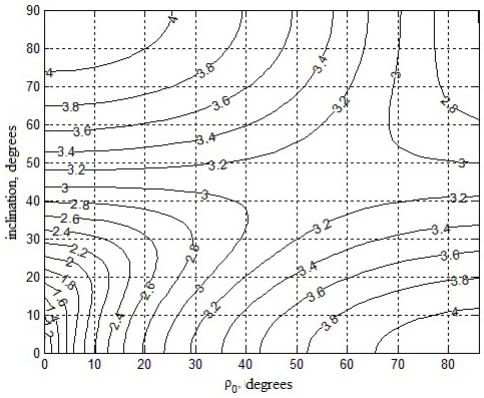

Fig. 18. Angular momentum after 5 orbits

Figure 18 ($\varepsilon = 0.1$, $\theta_0 = 1^\circ$) brings the effect of ρ_0 and i on the time-response. For small ρ_0 raising the inclination results in the time-response rise, for ρ_0 close to 90°, the time-response falls with orbit inclination rise. However, high inclined orbit is preferable again since there is no risk of extremely low time-response.

Equatorial component of angular velocity does not rise, its derivative is

$$\frac{d\left(l\sin\theta\right)}{du}=\varepsilon\left[-2+2p+\left(1-3p\right)\sin^2\rho\right]\sin\theta\cos\theta\,.$$

Since θ is close to 0 equatorial component lowers. Note that the nutation damping algorithm may be implemented simultaneously with the spinning algorithm.

6. Fine sun-pointing

The algorithm (4.8) may be used for fine sun-pointing. It is analyzed in paper [1] and it is shown that high-inclined orbit is definitely better for this algorithm to be implemented after the satellite is almost purely spinned. Here we have some numerical simulation results showing its accuracy.

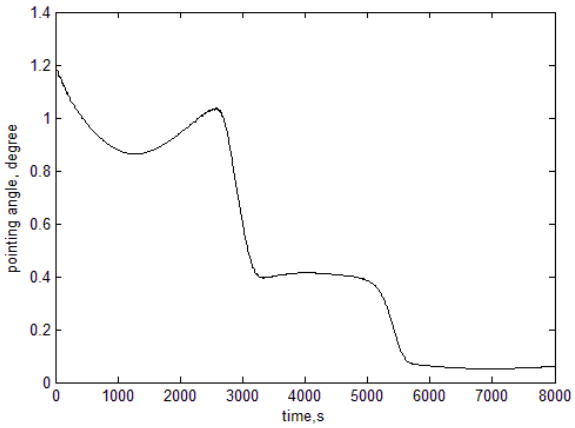

Figure 19. Pointing accuracy.

- Initial Euler angles are $\alpha=\alpha_s+1.2°$, $\beta=\beta_s+1.2°$, $\gamma=\gamma_s-61.3°$
- Initial pointing error is 1.175˚
- Angular rates $\omega_x=\omega_y=0$, $\omega_z=10°/s$
- Damping and reorientation gains are $k_1=5\cdot10^7 kg\cdot m^2/T\cdot s$, $k_2=10^6 kg\cdot m^2/T\cdot s^2$.

It is seen from figure 19 that fine sun-pointing algorithm allows precise orientation of the order of 10^{-1} degree (see figure 16 also).

Instead of (4.8) the torque constructed on the basis of PD-controller may be used. The simulations ran with previous algorithms underline how the necessary use

of a nutation damper in combination with the pointing algorithms provides a pointing accuracy strongly dependant on initial conditions and needing a careful tuning of gains (compare figures 8 and 13).

Other well-known control laws might be used in order to achieve a more precise and reliable pointing but the actuation is not always granted: in fact according to the nature of magnetic control, no arbitrary torques can be achieved, but only the components in the plane perpendicular to magnetic field vector.

This problem, indicated in literature as "underactuation", can be limited using in each instant the closer dipole moment to the theoretical one. So although commanded dipole is not exactly the required one in each instant, it is possible to use the closer one, selected using an optimization method (pseudo-inverse method).

Empirical result shows as for high-inclination orbits the underactuation problem is not so limiting: the reason is that the magnetic field orientation greatly changes along the orbit, so the probability of having a persisting underactuated axis is rather low.

So, in this case a simple PD-controller is used in order to show how to achieve the pointing of a spinned satellite is possible even with non-natively magnetic torques [12]. The control torque can be represented as

$$\mathbf{M}_{PD} = -\mathbf{K}_p\boldsymbol{\delta} - \mathbf{K}_d\dot{\boldsymbol{\delta}}$$

where $\mathbf{K}_p$ and $\mathbf{K}_d$ are gain matrices, proportional to the 3x3 unit matrix $\mathbf{I}_3$, $\mathbf{K}_p = k_p\mathbf{I}_3$ and $\mathbf{K}_d = k_d\mathbf{I}_3$, the pointing error is

$$\boldsymbol{\delta} = \arccos\left[(\mathbf{S}\mathbf{e}_3)\mathbf{S} \times \mathbf{e}_3\right].$$

The closer dipole providing a torque as close as possible to the wished one using a pseudo inverse method is

$$\mathbf{m}_{PD} = \frac{\mathbf{B}}{\|\mathbf{B}\|^2} \times \mathbf{M}_{PD}.$$

The resulting torque is the projection of $\mathbf{M}_{PD}$ on the plane perpendicular to $\mathbf{B}$. Simulations show how using this method an accurate pointing can be achieved and maintained even with the underactuation issue.

Figures 20-22 introduce results of numerical analysis of combined implementation of algorithms (4.1) and (4.5).

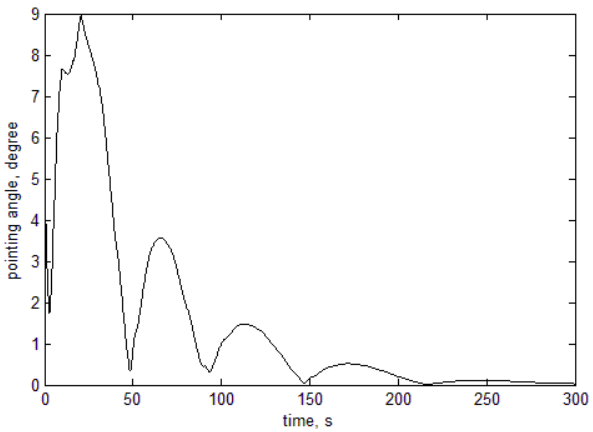

Fig. 20. Pointing angle evolution.

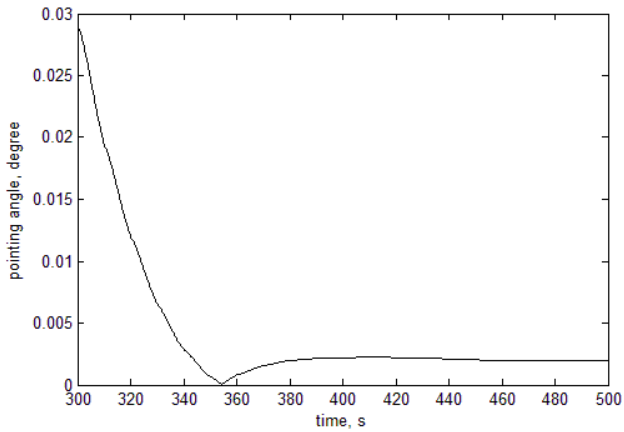

Fig. 21. Final pointing accuracy.

Figures 20 and 21 bring the pointing accuracy of the PD-controller implemented by magnetic coils. The accuracy is of order of 10^{-3} degree.

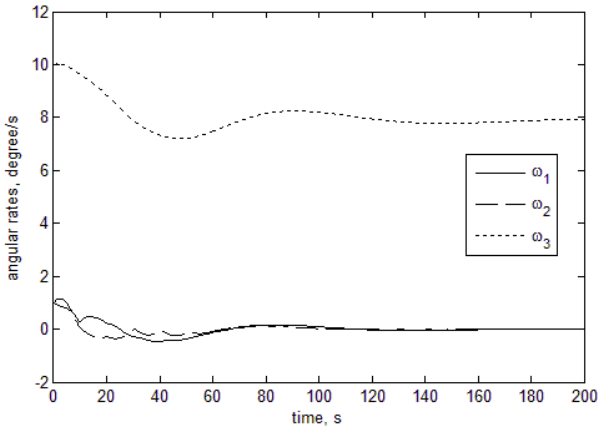

Fig. 22. Angular velocity rate

Figure 22 shows nutation damping when implementing both PD-controller algorithm and nutation damping. It is seen that spinning is decreased slightly but without any unnecessary effects. Initial conditions are as follows:

- Initial Euler angles are $\alpha = \alpha_s + 1.3°$, $\beta = \beta_s + 1.4°$, $\gamma = \gamma_s - 61.3°$
- Initial pointing error is 4.8˚

- Angular rates $\omega_x = \omega_y = 0$, $\omega_z = 10° / s$
- Damping and reorientation gains are $k_1 = 5 \cdot 10^7 kg \cdot m^2 / T \cdot s$, $k_p = 10^{-2} kg \cdot m^2 / s^2$, $k_d = 10^{-2} kg \cdot m^2 / s$.

Conclusion

A spin-stabilized satellite equipped with active magnetic attitude control system is considered. Satellite is reoriented to the required attitude of the axis of symmetry in the inertial space. Attitude control system implements six algorithms: nutation damping, two coarse reorientation algorithm, spinning and two fine reorientation algorithms. For each algorithm the time-response with respect to the orbit inclination and other system parameters is studied. Equations of motion are solved in quadratures using averaging technique. Analytic results show that the magnetic attitude control system time-response rises when orbit inclination is rather high. It is shown that simultaneous implementation of coarse reorientation algorithm and nutation damping algorithm leads to the satellite being reoriented to the accuracy of few degrees. This scheme allows faster reorientation than continuous detumbling and reorientation. Fine sun-pointing algorithm constructed on the basis of PD-controller is proposed, numerical analysis is carried out.

Acknowledgements

The study is carried out by partial support of Russian Foundation for Basic Research. We are especially gratefull to Prof. Filippo Graziani and mrs. Chantal Cappelletti for their continuous support and important remarks on the paper.

References

1. Ovchinnikov M.Y., Roldugin D.S., Pen'kov V.I. Analytical study of a three-stage magnetic attitude control to change a single-axis orientation // 62th IAC Congress, Paper IAC-11.C1.5.6. Cape Town, 2011. p. 11.

2. Shigehara M. Geomagnetic attitude control of an axisymmetric spinning satellite // Journal of Spacecraft and Rockets. 1972. V. 9. № 6. p. 391-398.

3. Renard M.L. Command laws for magnetic attitude control of spin-stabilized earth satellites // Journal of Spacecraft and Rockets. 1967. V. 4. № 2. p. 156-163.

4. Shrivastava S.K., Modi V.J. Satellite attitude dynamics and control in the presence of environmental torques – a brief survey // Journal of Guidance, Control, and Dynamics. 1983. V. 6. № 6. p. 461-471.

5. Beletsky V.V., Novogrebelsky A.B. Occurence of Stable Relative Equilibrium of a Satellite in Model Magnetic Field // Astronomical Journal. 1973. V. 50. № 2. p. 327-335.

6. Beletsky V.V. Motion of a Satellite about its Center of Mass in the Gravitational Field. Moscow: MSU publishers, 1975.

7. Stickler A.C., Alfriend K.T. Elementary Magnetic Attitude Control System // Journal of Spacecraft and Rockets. 1976. V. 13. № 5. p. 282-287.

8. Beletsky V.V., Khentov A.A. Tumbling Motion of a Magnetized Satellite. Moscow: Nauka, 1985.

9. Grebenikov E.A. Averaging in Applied Problems. Moscow: Nauka, 1986.

10. Grahn S. An On-Board Algorithm for Automatic Sun-Pointing of a Spinning Satellite // Swedish patent application n. 9702333-7.

11. Handbook of Mathematical Functions: with Formulas, Graphs, and Mathematical Tables / editors M. Abramowitz, I.A. Stegun. New York: Dover, 1972. ed. 9.

12. Sedlund C.A. A simple sun-pointing magnetic controller for satellites in equatorial orbits // IEEE Aerospace conference. Big Sky, Montana, 7-14 march 2009. p. 1-12.

Contents